

Article

Development of Decay in Biofilms under Starvation Conditions—Rethinking of the Biomass Model

Michael Cramer *  and Jens Tränckner 

Department of Water Management, University of Rostock, 18059 Rostock, Germany;
jens.traenckner@uni-rostock.de

* Correspondence: michael.cramer@uni-rostock.de

Received: 27 March 2020; Accepted: 25 April 2020; Published: 27 April 2020



Abstract: The study investigates the decay of heterotrophic biomass in biofilms under starvation conditions based on measurements of the oxygen uptake rate (OUR). Original incentive was to understand the preservation of active biomass in SBR-trickling filter systems (SBR-TFS), treating event-based occurring, organically polluted stormwater. In comparison with activated sludge systems, the analyzed biofilm carrier of SBR trickling filters showed an astonishing low decay rate of 0.025 d^{-1} , that allows the biocenosis to withstand long periods of starvation. In activated sludge modeling, biomass decay is regarded as first order kinetics with a 10 times higher constant decay rate ($0.17\text{--}0.24 \text{ d}^{-1}$, depending on the model used). In lab-scale OUR measurements, the degradation of biofilm layers led to wavy sequence of biomass activity. After long starvation, the initial decay rate (comparable to activated sludge model (ASM) approaches) dropped by a factor of 10. This much lower decay rate is supported by experiments comparing the maximum OUR in pilot-scale biofilm systems before and after longer starvation periods. These findings require rethinking of the approach of single-stage decay rate approach usually used in conventional activated sludge modelling, at least for the investigated conditions: the actual decay rate is apparently much lower than assumed, but is overshadowed by degradation of either cell-internal substrate and/or the ability to tap “ultra-slow” degradable chemical oxygen demand (COD) fractions. For the intended stormwater treatment, this allows the application of technical biofilm systems, even for long term dynamics of wastewater generation.

Keywords: activated sludge; ASM; modelling; oxygen uptake rate OUR; respirometry; silo facility; trickling filter

1. Introduction

Biological wastewater treatment is based on the accumulation of a complex consortium of microorganisms in suspended systems (activated sludge), as biofilms attached to carriers (biofilm systems), or a combination of both. Provided optimal living conditions and substrate supply, the performance of those systems is mainly dependent on mass of metabolic active microorganisms. In situations with strongly varying loading (e.g., periodic wastewater generation, treatment of organic polluted stormwater), the varying substrate supply can lead to strong variations of active biomass and related substrate transformation rates. Especially long starvation conditions may lead to a significant decrease of performance due to biomass decay. This needs to be assessed when designing treatment technologies for those conditions.

Bacteria (as the most relevant group for substrate metabolism in activated sludge and biofilm systems) apply various adaptation strategies to starvation. The most prominent are altering the macromolecular composition [1,2] and reducing the cell size [3,4]. Besides, a reduction of the protein synthesizing system, the ribosomes, has been observed. This process, known as ribophagy is so far

not completely understood, but simplified, the degradation of ribosomes seems to serve as a source of energy supply [3,5,6]. It can be postulated that periodic changing substrate supply will perform a selective pressure on the biocenosis and define the phenotypic state of the bacteria [7]. However, these complex starvation-survival response strategies of bacteria can hardly be considered when describing biologic wastewater treatment mathematically.

Instead, the extensive variety of organism groups and their individual response to the environment needs to be streamlined, the governing biological processes, which again can only be described in a strongly simplified way. Currently, mathematical modeling of aerobic biologic wastewater treatment is based on the concepts developed in the activated sludge models [8]. This also applies for biofilm systems with additional challenge of describing matter transport through the biofilm and related formation layers with different environmental conditions and processes [8–10]. In activated sludge modelling (ASM), the variety of heterotrophic bacteria families is summarized in these models as one group (X_H), expressed as chemical oxygen demand (COD).

The dynamics of heterotrophic biomass and the associated COD degradation are mostly mathematically described by combining growth and decay kinetics, both with a first order dependence on active biomass. Regarding decay, two different approaches were proposed and alternatively applied in activated sludge and biofilm modeling: (i) endogenous respiration model [11,12] and (ii) the death-regeneration model [13–15].

In the first commonly used endogenous respiration approach as shown in Figure 1, the active biomass can be directly consumed for providing maintenance energy for microorganisms as a consequence of decay [11]. As result of decay, a fraction (f_u) remains as endogenous residue X_E .

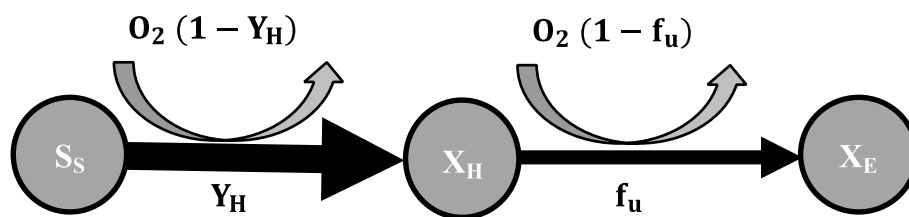


Figure 1. Principle of the endogenous respiration model.

The death-regeneration model was introduced by Dold, Ekama, and Marais (1980). In this approach, heterotrophic microorganisms are releasing an unbiodegradable endogenous residue fraction X_E and a biodegradable COD fraction X_S during decay, which is then consumed by an organism, justifying oxygen consumption under starvation conditions (Figure 2). As a by-product of these decayed bacteria and, therefore, released bioavailable X_S fraction, new growth is obtained, which is called regeneration. With this approach, increasing respiration rate after anaerobic periods can firstly be explained with the substrate release as a consequence of decay. If decay is an independent process, it would not stop under anaerobic conditions and, therefore, the substrate would accumulate, which then can be oxidized under aerobic conditions.

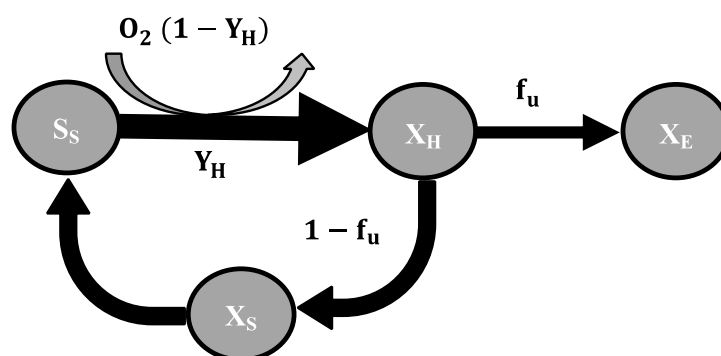


Figure 2. Principle of the death-regeneration model.

According to this model, the decay rate b_H must become larger than in the endogenous respiration approach to compensate for regeneration. The decay rate from the respiration model b' can be converted to the death-regeneration model with Equation (1): for this, an endogenous residue factor f_U of 0.08 was assumed [13].

$$b = \frac{b'}{1 - Y_H \cdot (1 - f_U)} \quad [\text{d}^{-1}] \quad (1)$$

where Y_H is the heterotrophic biomass yield, b and b' is the decay rate within the death-regeneration and endogenous respiration approach, respectively. Applying the proposed biological constants of ASM [12], the corresponding decay rate for domestic wastewater is $b = 0.62 \text{ d}^{-1}$ and $b' = 0.24 \text{ d}^{-1}$.

A simple and well-established method to evaluate the activity of heterotrophic microorganism X_H is measuring the respiration rate, expressed as biological oxygen uptake rate (OUR). With slight variations, the same method is commonly used for various research questions [16–19]. In the state of the art, OUR is measured with respirometers under strictly controlled conditions to avoid side-effects. The magnificent advantage of this method is highly time resolved and low-cost measuring of kinetic parameters and COD fractions as it is just based on measuring dissolved oxygen. Figure 3 shows in a schematic way the conversion of COD fraction in the raw water (left) and into biomass (right) during the biological process. The influent $\text{COD}_{h,\text{in}}$ can either be degraded, which can be measured with the oxygen respiration rate for degradation OUR_{deg} or incorporated into biomass as excess sludge X_{ES} .

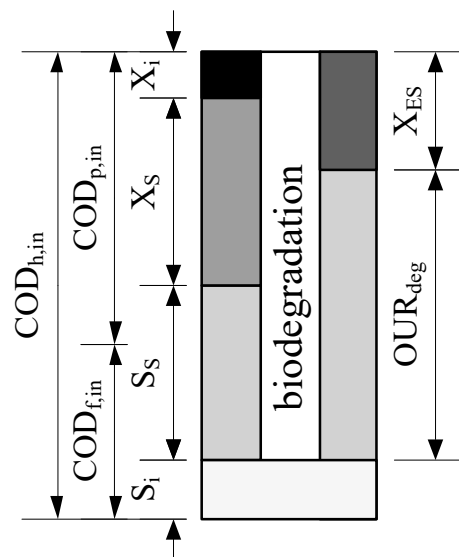


Figure 3. Chemical oxygen demand (COD) fractions during biological treatment [20].

For a long time it had been generally assumed that the decay rate is a constant and independent from substrate supply conditions (expressed for activated sludge systems by the sludge retention time SRT) for the particular biological environmental [8,11,18,21]. Besides, the endogenous residue fraction X_E and yield coefficient for heterotrophic organism Y_H is regarded to be constant for a particular substrate in the ASM. These are rather mechanistic assumptions and only valid for systems with rather low load variations. Current research in activated sludge systems proved that both the X_E fraction [22] and the decay rate b_H [23] are a function of sludge retention time SRT (i.e., function of substrate supply). Due to this observation at extreme conditions of low COD, the question arises if organisms can adapt their decay rate and the assumption of a constant decay rate has to be reconsidered or if the existing ASM has to be extended with an additional very slowly degradable COD fraction (consisting of “hard” external COD and/or cell-internal reserves) and according degradation process. Consequently, this would mean that the actual decay leading to cell death would occur at a lower rate than previously calculated. This is important for the activity and sludge production of all systems running with permanent or periodically occurring starvation conditions.

Those conditions occur for example in systems that treat rainwater runoff with high organic pollution. A practical application is stormwater-runoff from agricultural silo facilities which can be heavily contaminated by organic and nutrient pollutants and has to be treated before discharge into surface waters [24]. In contrast to domestic wastewater, the inflow to a treatment facility is rain dependent with dry weather periods of several weeks to months. Although, storage devices prior to a treatment plant can dampen these dynamics and biologic treatment systems should be able to survive starvation periods of several weeks and recover quickly in case of rain events. Attached growth systems are for those conditions interesting as they combine rather simple and robust technology with a certain ability to cope with load dynamics [25,26].

Applied to the original question, the development of active heterotrophic biomass (here, in attached growth systems) under long lasting starvation conditions, the main objectives of this paper are

- The quantification of cell-decay rate under starvation conditions;
- To identify and quantify degradation of a “new” COD fraction, made accessible under those conditions;
- To quantify the recovery of the biofilm after starvation.

To verify the results achieved under lab-scale conditions a pilot plant for treating stormwater runoff with high organic pollution is operated, accordingly.

2. Material and Methods

2.1. Design of Wastewater Treatment Plant

Stormwater-runoff and silage effluent of a biogas plant was treated by an SBR trickling filter system (SBR-TFS) which is based on a trickling filter and a secondary clarification and storage tank. A compact description is given here. The entire process of SBR trickling filter is discussed in [27].

Figure 4 shows a principle schema of the treatment system. In contrast to conventional trickling filters (see e.g., [28]), the SBR-TFS is operated as a sequence-batch-reactor (SBR) to allow anaerobic phases for a systematic nutrient removal. Like typical SBR as known from activated sludge systems (ASS), the process is divided into an anaerobic and aerobic step. The anaerobic step acts as an upstream denitrification. During this step, the trickling filter is firstly fed with stormwater-runoff from the combined retention and primary clarification tank (rich in COD, ammonia, and phosphorous) and distributed with a rotary sprayer for a homogeneous spread all over the surface. After dosage, the trickling filter is filled up with treated water from the combined storage and secondary clarification tank (containing nitrate from the previous cycle) to the highest level to avoid oxygen diffusion during anaerobic recirculation (step 2b). The completely ponded system is then internally recirculated to achieve denitrification (and anaerobic P-release, if enhanced biological removal shall be performed). The aerobic phase follows the anaerobic phase in which the wastewater in the trickling filter is emptied into the storage tank. In this phase, the trickling filter sump is constantly pumped into the storage tank and back to the rotary sprayer of the trickling filter until COD degradation and nitrification are completed (step 3b). Distributing the water over a high surface area of the biofilm carrier provides a sufficient oxygen supply through diffusion. The final step is the sedimentation, separating the activated sludge from the clarified water, which is finally discharged.

For the decay experiments, a small-scale SBR-TFS was operated. The steps of one SBR cycle including anoxic, anaerobic, and aerobic conditions are presented in Figure 5. The total volume of the trickling filter was 80 L with a packing bed volume of 54 L and a specific surface area of the biofilm carrier of $322 \text{ m}^2 \cdot \text{m}^{-3}$. During the starvation period, no stormwater was added and the SBR-TFS was only operated with the same treated wastewater.

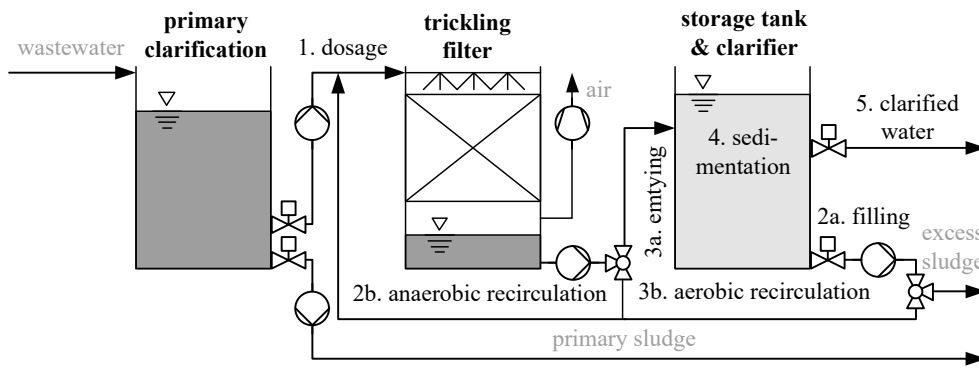


Figure 4. Principle schema of the trickling filter system [27].

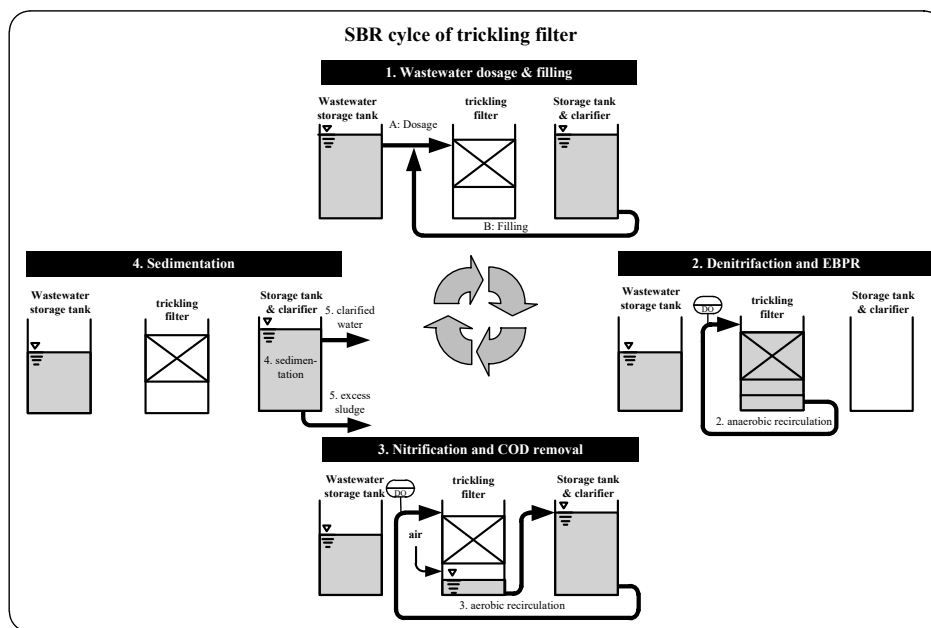


Figure 5. Steps of one SBR cycle [27].

2.2. Analytical Procedure

For measuring the decay rate of attached growth system, a modified OUR method was used for aerobic respiratory in laboratory scale. The schema is presented in Figure 6, left. OUR tests have been developed and widely applied for activated sludge systems [12,29]. In order to meet the conditions in the SBR-TFS system closely, activated sludge was replaced by 13 biofilm carrier fixed on a line in a 1 L reactor filled with tap water. The carriers were taken from the pilot plant described above, which was operated for 6 months to treat stormwater-runoff from a biogas plant. A magnetic stirrer provided a homogenous mixture. The dissolved oxygen DO was measured with an optical DO probe (time resolution: 1 s) and controlled in a range of 2–4 g m⁻³. OUR was calculated for each switch-off phase by a linear regression of the declining DO. During the starvation period, the reactor filled with biofilm carriers was aerated without substrate supply. From the resulting respirogramm during starvation, the endogenous respiration rate OUR_e was calculated according to [20], (see “mathematical model” below, Section 2.3).

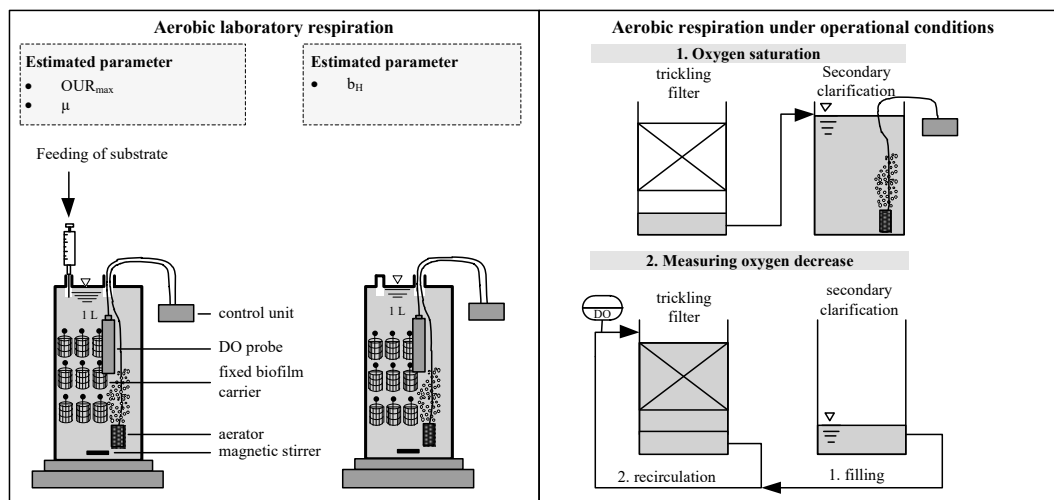


Figure 6. Schema of the respirometry measurement of the oxygen uptake rate.

For measuring maximum growth rates, the bacteria were fed with silage effluent as highly degradable substrate [20]. The substrate was injected into the reactor after 3, 4, 7, and 13 days of continuous starvation. After each dosage, the starvation period started again. After substrate dosage, the maximum respiration rate OUR_{max} was calculated from the respirogramm in the same way as OUR_e . Assuming a typical value for f_U and a substrate specific yield coefficient, the growth rate can be calculated from the endogenous and maximum OUR according to the mathematical model, described below.

In addition to the laboratory respiration tests, the oxygen consumption was measured in the pilot-scale trickling filter (Figure 6, right). To allow ponding, the aeration aperture at the bottom of the trickling filter is connected to a riser pipe, ending above the highest filling level. At aerobic conditions the same pipe is empty and provides air supply. To avoid unintended limitation of aeration, a fan on top of the rising pipe is sucking air through the unsubmerged trickling filter. For measuring the OUR in the trickling filter, an optical DO probe was installed in a measuring section of the recirculation pipe shortly before the rotary sprayer. The OUR measurement was performed in three succeeding steps: (1) the treated wastewater in the secondary clarification was aerated to oxygen saturation with an external aerator. (2) The oxygen saturated water was pumped to the trickling filter to the upper level. To minimize oxygen diffusion, the rotary sprayer was temporary replaced with a pipe that plunged into the water. (3) The water in the filled-up trickling filter was recirculated and the oxygen decline was recorded. This procedure results in one single OUR measuring point and was repeated each 2 days.

2.3. Mathematical Model

For mathematical derivation of endogenous decay rate based on the OUR method, see [20]. For endogenous respiration, OUR corresponds to the change of X_H , reduced by an endogenous residue factor f_U :

$$OUR_e = (1 - f_U) \cdot \frac{dX_H}{dt} \left[g \cdot m^{-3} \cdot d^{-1} \right] \quad (2)$$

The net growth of heterotrophic bacteria X_H is the difference of growth and decay. Both growth and decay can be described as first order kinetics of actual biomass concentration. Additionally, there is a substrate dependency for the growth, usually expressed by a Monod kinetics (Equation (3)).

$$\frac{dX_H}{dt} = \mu_{max} \cdot \frac{S}{K_S + S} \cdot X_H - b_H \cdot X_H \left[g \cdot m^{-3} \cdot d^{-1} \right] \quad (3)$$

where b_H is the decay rate of heterotrophic organism, μ is the bacteria growth rate, S is the substrate concentration, and K_S is the substrate saturation coefficient.

The bacteria growth is stoichiometrically linked to the oxygen demand Equation (4):

$$\text{OUR}_{\text{growth}} = \mu_{\text{max}} \cdot \frac{1 - Y_{\text{H}}}{Y_{\text{H}}} \cdot X_{\text{H}} \left[\text{g} \cdot \text{m}^{-3} \cdot \text{d}^{-1} \right] \quad (4)$$

Substrate utilization results in oxygen consumption with respect to bacteria growth and endogenous respiration. With this in mind, the maximum oxygen consumption rate OUR_{max} at time $t(0)$ can be determined with Equation (5):

$$\text{OUR}_{\text{max}}(0) = \left(\mu_{\text{max}} \cdot \frac{1 - Y_{\text{H}}}{Y_{\text{H}}} + (1 - f_{\text{U}}) \cdot b_{\text{H}} \right) \cdot X_{\text{H}} \left[\text{g} \cdot \text{m}^{-3} \cdot \text{d}^{-1} \right] \quad (5)$$

Substituting X_{H} in Equation (5) by the rearranged Equation (2) results in:

$$\text{OUR}_{\text{max}}(0) = \left(\mu_{\text{max}} \cdot \frac{1 - Y_{\text{H}}}{Y_{\text{H}}} + (1 - f_{\text{U}}) \cdot b_{\text{H}} \right) \frac{\text{OUR}_{\text{e}}(0)}{(1 - f_{\text{U}}) \cdot b_{\text{H}}} \left[\text{g} \cdot \text{m}^{-3} \cdot \text{d}^{-1} \right] \quad (6)$$

Equation (6) can be arranged to calculate the maximum growth rate from respirometry:

$$\mu_{\text{max}} = \frac{Y_{\text{H}}}{1 - Y_{\text{H}}} \cdot (1 - f_{\text{U}}) \cdot b_{\text{H}} \cdot \left(\frac{\text{OUR}_{\text{max}}(0)}{\text{OUR}_{\text{e}}(0)} - 1 \right) \left[\text{g} \cdot \text{m}^{-3} \cdot \text{d}^{-1} \right] \quad (7)$$

The substrate specific yield coefficient Y_{H} of silage effluent was separately determined with 0.87 [20]. This rather high yield is attributable to its sugar-like ingredients as glucose have a yield coefficient of 0.90–0.91 [30]. The decay rate b_{H} was calculated from the respirogram and for f_{U} , a typical value of 0.2 for heterotrophic biomass was assumed [12].

3. Results

3.1. Decay Rate During Starvation

Typically, the decay rate of heterotrophic organism is graphically expressed as a logarithmical decrease of endogenous respiration for activated sludge system. However, for the investigated attached growth systems, this is hardly applicable as Figure 7 shows. The time series shows that repeatedly a logarithmical decrease of on average 15 h is followed by an exponential increase of on average 10 h with continuously decreasing amplitude. As the used biofilm carrier were grown with a thick biofilm, it seems that the organism makes organic compounds inside the biofilm stepwise accessible as substrate. The processes leading to periodic OUR increase are not clear yet. Working hypotheses are (i) hydrolysis of slowly degradable substrate in the biofilm and decay products, (ii) usage of intracellular storage of the organisms themselves and ribophagia or a combination of both. Layering and diffusional processes may be influencing, too [31,32].

According to the black line in Figure 7, the best model fit for endogenous decay rate during the time period of OUR decrease at the beginning of the experiment is the recommended decay rate of 0.24 d^{-1} as widely applied and proved in activated sludge modelling (ASM1) [21]. Considering both parts of the wavy respirogram, the decreasing and increasing OUR, a net decay rate $b_{\text{H}+\text{stor}}$ of 0.17 d^{-1} in accordance with ASM3 would fit best for a certain time period, here 6–7 days. To express this switch of decay rate, the apparent OUR under endogenous condition is divided into OUR obtained by degradation of an additional fraction X_{US} (gray dot pointed line, Figure 7) and OUR obtained by base decay rate b_{H} of active biomass (black dot pointed line, Figure 7). The total OUR is therefore the sum of both (gray dotted line). After this time period, the modelled net decay rate changes significantly to a lower value of 0.025 d^{-1} , nearly a tenth of the conventionally applied decay rates. From this time on, all storage fractions are consumed and the sole decay rate is obtained (black dot pointed line).

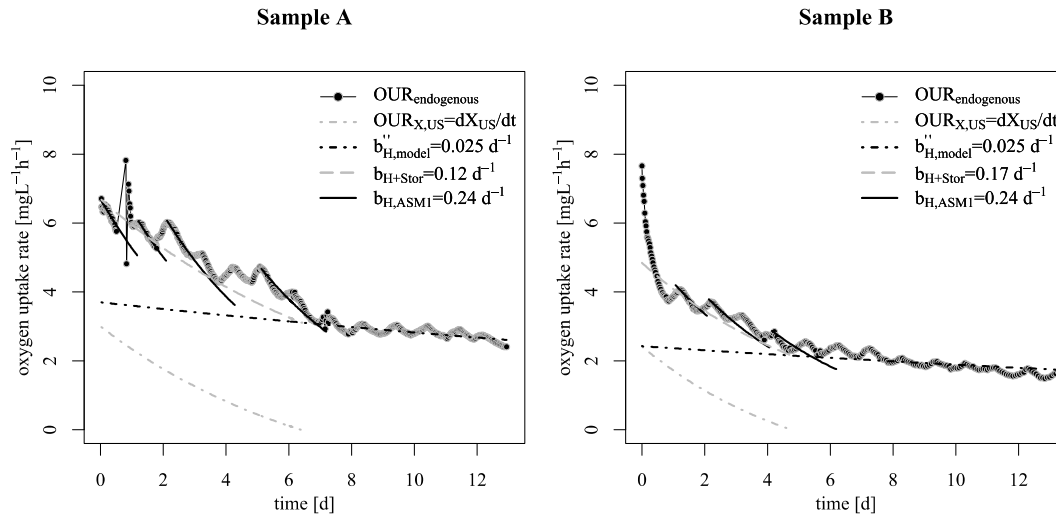


Figure 7. Alternation of decay rate during starvation of biofilm carrier.

If the proposed concept of a base decay and a degradation of “ultra-slowly” degradable X_{US} applies, the net decay rate after substrate feed as sum parameter of decay and X_{US} degradation should be the same as in the beginning of the experiment (0.17 d^{-1}) and then fall back to the base decay rate b_H as soon as this additional storage fraction is consumed (0.025 d^{-1}). To answer this, substrate was fed in excess to ensure an accumulation of X_{US} after 18 days of starvation. As Figure 8 shows, the brutto decay rate b_{H+stor} increased again from 0.025 (before day 18) to 0.17 d^{-1} after substrate feed. After complete consumption of X_{US} , the decay rate during OUR decreased to 0.025 d^{-1} once more ($=b_H$). Precisely, degradation of an addition fraction extended the base decay rate b_H by this storage fraction, which can be expressed again with the degradation rate b_{H+stor} . Hence, the best model fit for modelling the overall process for the base decay rate is 0.025 d^{-1} in addition with a consumption rate ($=b_{H+stor}$) for X_{US} of $0.17\text{--}0.025\text{ d}^{-1}$. This shows that the alternation is only temporary and therefore can be related with an additional degradation process of the new fraction X_{US} .

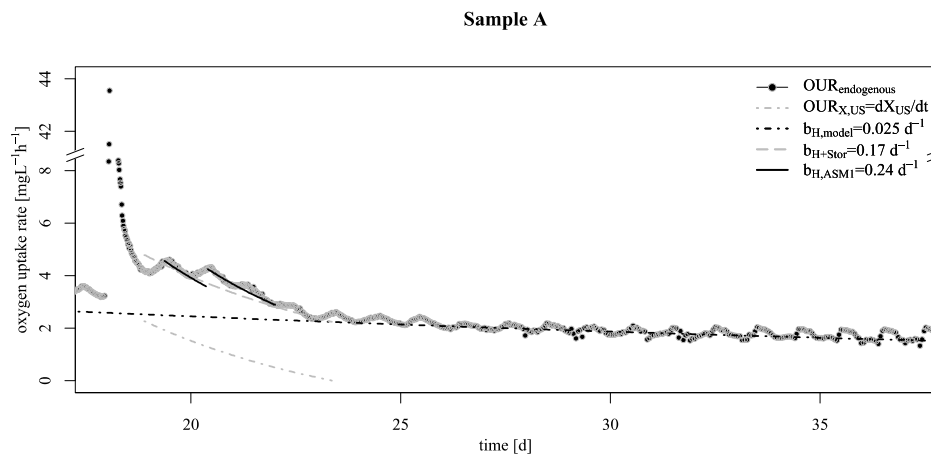


Figure 8. Results of endogenous OUR after substrate feeding.

3.2. Verification of the Low Decay Rate in Pilot Scale

The validity of at least two decay mechanisms—(1) a fast decay rate controlled by the availability of an additional X_{US} fraction and (2) a base decay rate in “real” starvation conditions—should be provable under operational conditions of the pilot plant. The proof can be performed with two experimental concepts: (i) decline of the “operational” OUR under starvation conditions and (ii) measuring maximum biomass activity after starvation. The latter experiment assumes that the identified base decay rate

should preserve the biomass activity on a much higher level than calculated with the commonly proposed decay rate.

According to the schema of Figure 6 on the right, respirometry measurements were performed in the pilot plant. For this, the wastewater in the storage tank was aerated until oxygen saturation occurred and filled back to the highest level in the trickling filter. After filling, the inner recirculation was started to measure the dissolved oxygen decrease within the trickling filter. This decrease lasts up to 3 h, depending on the prior starvation period and the associated endogenous respiration rate (Figure 9). The figure illustrates the parametrized sequencing decay model after 9 days of starvation. Until the fourth day of starvation, the best model fit is a net decay rate of 0.14 d^{-1} , including degradation of “ultra-slow” degradable COD fraction X_{US} (gray dotted line) and pure decay (black dotted line). At this point, X_{US} is consumed and the decay rate decreases to the base decay rate of 0.022 d^{-1} . Separating both processes would yield a decay rate for the storage products of 0.14 d^{-1} (-0.022 d^{-1}). In conclusion, the results show that the findings of a low decay rate are indeed representative under real operational conditions for treating stormwater-runoff from silo facilities.

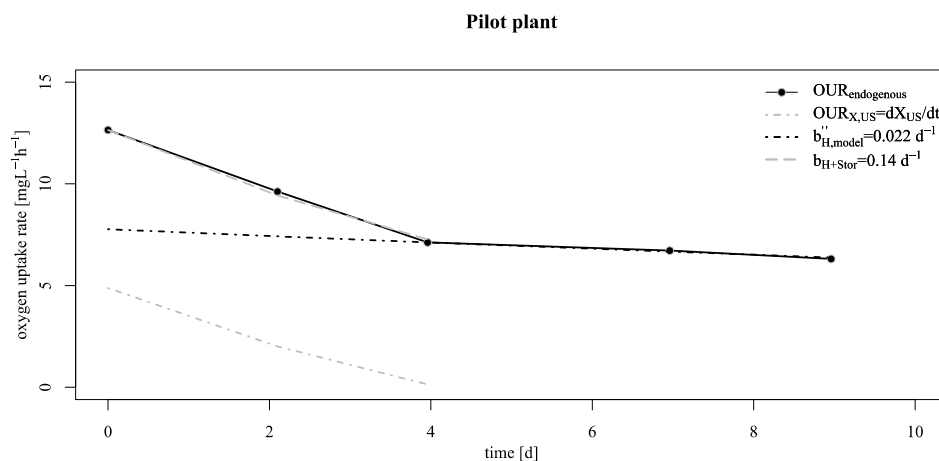


Figure 9. Results of respirometry measurement in a pilot scale trickling filter.

Under starvation conditions, the decrease of OUR_{max} represents (according to Equation (5)) directly the reduction of active biomass X_H . Knowing the initial $OUR_{max}(0)$ and decay rate b_H , OUR_{max} at certain times of starvation can be calculated with Equation (8):

$$OUR_{max,calc.}(t) = OUR_{max}(0) \cdot e^{-b_H \cdot t} \left[g \cdot m^{-3} \cdot d^{-1} \right] \quad (8)$$

For this, silage effluent was dosed into the reactor after 5, 8, and 13 days of continuous starvation as depicted in Figure 10. As shown in Figure 10 on the left, the observed and calculated OUR_{max} according to Equation (8) are nearly the same even after 13 days of continuous starvation. Therefore, it can be inferred that the decay rate of about 0.025 d^{-1} is true and is suitable for an adequate prediction of biomass decrease under long starvation periods. The respirogramm for the case of 13 days of continuous starvation is shown in Figure 10 on the right. Based on the measurements of OUR_e and OUR_{max} and considering Equation (7), a growth rate μ_{max} of 7.9 d^{-1} results at a constant Y_H and f_U at a temperature of $25 \text{ }^\circ\text{C}$. However, with respect to typical growth rates of 6 d^{-1} at $20 \text{ }^\circ\text{C}$, a growth rate of approximately 8.5 d^{-1} would be expected. Therefore, the estimated rate is within the expected range.

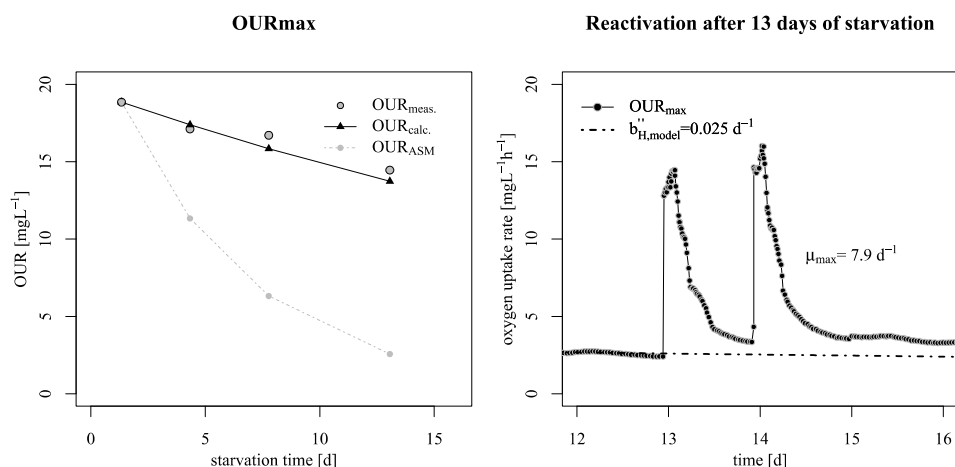


Figure 10. Reactivity of microorganism after starvation.

4. Discussion

The results showed that long starvation periods in the investigated biofilms are linked to a significant lower decay rate of just a tenth of the recommended decay rate used in the ASM [12]. Experiments with activated sludge support these findings [22,23]. Actually, both decay rate and particulate inert fraction are rather a function of nutritional state than a constant. For rather steady state substrate supply as common in domestic wastewater treatment plants, this functional relationship is neither detectable nor relevant. However, for long or permanent extreme starvation conditions, the approach of the ASM is not sufficient to explain an alternation of the decay rate. This limitation could be overcome by slight changes of the modelling concept. The actual decay (as irreversible die-off of biomass) needs to be described with the observed much lower decay rate, but is superimposed by decay of “ultra-slow degradable” substrate X_{US} , which is not “tapped” under normal conditions. The identity of X_{US} is not clear yet. It can be thought as (i) cell internal reserve substrate or (ii) hardly accessible external substrate or a mix of both. From a modelling perspective, taking it as external substrate is the simplest approach, since X_{US} formation is in this case decoupled from bacterial growth. This conceptual idea could also explain the wavy decline of decay, especially if combined with the death-regeneration approach. Transformation processes within the rather thick biofilm used in our experiments were probably diffusion controlled and oxygen limited in deeper layers. The diffusion limitation and oxygen penetration into the biofilm are presented in the Supplementary Materials. However, in the death-regeneration approach, decay is defined to be independent from oxygen supply. Therefore, independent from the aerobic state, biodegradable fractions are released by decay of organism but not used due to oxygen limitation. The biodegradable fractions are preserved in the inward layer of the biofilm carrier. The preserved COD fractions in the lower layers would lead to an increased respiration rate as soon as the upper layer is fully decayed. This short-term regrowth is followed by aerobic decay of the newly formed biomass, leading to the wave-like behavior of the observed respiration rates. This layering effect causing diffusion limitations is often associated with a simultaneous nitrification and denitrification in biofilm systems [27,33]. In contrast to the biofilm experiments in this study, experiments with activated sludge will probably not allow such a clear distinction between decay of X_{US} and actual decay of biomass due to the stochastic distribution of both fractions. Accordingly, respirometry measurement would show a more continuous adaptation of the decay rate.

The extension of the death-regeneration approach by an “ultra-slow” degradable X_{US} fraction as an external substrate is illustrated in Figure 11. It can be made available via hydrolyzation to a slow degradable fraction $(1 - f_E)$ and is then consumed as S_S . A small ratio f_E remains as endogenous residue X_E . The hydrolyzation itself is poorly understood, yet, due to the variety of substrates and apart from this, the experiments in the literature are mainly accomplished with pure substrates [34].

Most model concepts (for instance ASM1, ASM2d, ASM3) are based on a one step hydrolyzation. In the approach proposed here, the X_{US} fraction is firstly hydrolyzed into X_S and further hydrolyzed into S_S . However, X_{US} hydrolyzation is inhibited by the concentration of the better accessible X_S and will only be degraded under real starvation conditions when X_S is fully degraded. Once X_{US} is consumed, only the base decay rate is obtained. Mathematically, this can be considered with an inversed Monod kinetic (Equation (10)). The key idea behind this is that the term for X_{US} is “inactive” as long as X_S is still available (Equation (9) is above zero). With decreasing X_S , the term becomes more and more “active” and is most active when X_S drops to zero. Now, X_{US} becomes the limiting step measured in respirometry. As soon as X_{US} is degraded also, the term reaches zero and only the base decay rate is active (see Equation (7)).

$$\frac{dX_S}{dt} = X_H \cdot k_h \cdot \left(\frac{\frac{X_S}{X_H}}{K_S + \frac{X_S}{X_H}} \right) \left[g \cdot m^{-3} \cdot d^{-1} \right] \tag{9}$$

$$\frac{dX_{US}}{dt} = X_H \cdot k_h \cdot \left(\frac{\frac{X_{US}}{X_H}}{K_S + \frac{X_{US}}{X_H}} \cdot \frac{K_S}{K_S + \frac{X_S}{X_H}} \right) \left[g \cdot m^{-3} \cdot d^{-1} \right] \tag{10}$$

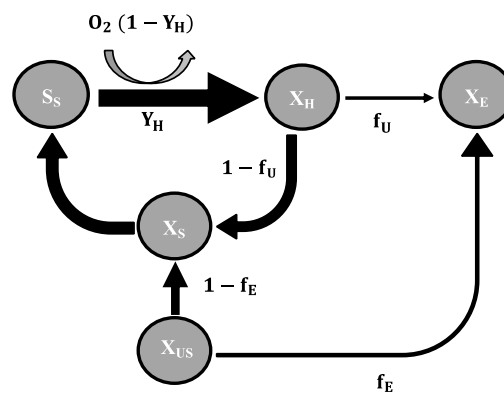


Figure 11. Extending of the death-regeneration model.

Similar to the death-regeneration approach, the endogenous approach can be extended in a similar way (Figure 12). Here, the possibility of a cell internal storage fraction was exemplarily used to integrate the additional X_{US} fraction. In this approach, the fast-degraded substrate during endogenous conditions (illustrated with a bold line) internal storage fraction X_{US} is directly degraded into the endogenous residue X_E , without prior hydrolysis. Both base decay and X_{US} consumption are running parallel. The degradation rate of X_{US} can be expressed as the sum decay rate of storage product and base decay rate b_{H+stor} discussed above minus the base decay rate ($b_{H+stor} - b_H$). The irreversible decay of active biomass is running in parallel with the observed much lower decay rate b_H (illustrated with a thin line). Summarizing, as long as X_{US} is still available as substrate, the brutto degradation rate b_{H+stor} is suitable as best model fit for describing the OUR decrease with time. As soon as X_{US} is fully degraded, the sole decay rate b_H is obtained.

$$\frac{dX_H}{dt} = -X_H \cdot b_H \left[g \cdot m^{-3} \cdot d^{-1} \right]. \tag{11}$$

$$b_H = 0.025 \text{ d}^{-1}$$

$$\frac{dX_{US}}{dt} = X_H \cdot k_h \cdot \left(\frac{\frac{X_{US}}{X_H}}{K_{US} + \frac{X_{US}}{X_H}} \right) = -X_H \cdot (b_{H+stor} - b_H) \left[g \cdot m^{-3} \cdot d^{-1} \right] \tag{12}$$

$$b_{H+stor} = 0.17 \text{ d}^{-1}$$

$$\frac{dX_E}{dt} = f_E \cdot X_{US} \cdot (b_{H+stor} - b_H) + f_U \cdot X_H \cdot b_H \quad [\text{g} \cdot \text{m}^{-3} \cdot \text{d}^{-1}] \quad (13)$$

$$f_U = 0.20$$

$$f_E = 0.48$$

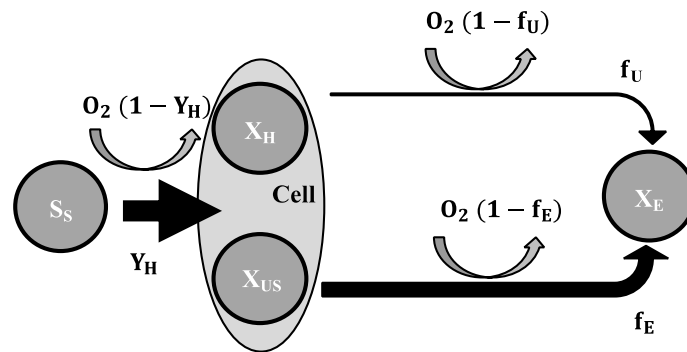


Figure 12. Adjusting of the endogenous respiration model.

A classification of X_{US} as a cell internal COD fraction or as an external fraction which can be made available to heterotrophic organism by a multi-step hydrolyzation depends on the model approach taken and can both be easily integrated. Compared to the complex adaptation of microorganisms to varying nutritional and environmental conditions, both approaches are still rather conceptual but would sufficiently describe the observed change of decay rate.

5. Conclusions

The aim of this work was to quantify the reduction of biomass activity in biofilm systems suffering from periodic starvation conditions. For this, two experimental approaches were combined: (i) OUR experiments with biofilm carriers taken from a pilot-scale trickling filter, (ii) adapted OUR experiments of the complete trickling filter. According to the findings of this work, the following conclusions are drawn:

- Starvation of biofilm carrier was characterized by wavy increase and decrease of endogenous respiration, ending at a surprisingly low base decay rate. Justifying this effect with either the existing death-regeneration model or the endogenous respiratory model is not a straightforward task;
- A possible explanation approach is the layering and the associated oxygen diffusion limitations, which preserves the lower layers from real degradation of COD but not from decay;
- However, even taking these biofilm specific conditions apart: the base decay rate is considerably lower than the recommended value in existing ASM;
- This lower decay rates allow a conservation of biological activity over long starvation periods as shown by reactivation experiments at the pilot SBR trickling filter;
- To explain these findings, the common one step decay model needs be divided into at least two processes: (i) a fast degradation of cell internal reserves and/or hardly degradable external COD, named here as “ultra-slow” degradable COD X_{US} and (ii) the net decay of active biomass;
- Based on recent publications, it can be assumed that these findings are transferrable to activated sludge systems;
- The findings have practical consequences for aerobic biologic reactors suffering from long starvation conditions: (i) they should survive those conditions better than commonly presumed, (ii) biomass production is larger and aeration demand is lower than commonly presumed.

These findings seem to unmask a so far not relevant simplification of biological processes leading to knowledge a gap between reality and the model [34]. It became only evident here, due to the changed

viewpoint of a new treatment challenge: intermittent runoff with high organic pollution. However, other investigations with activated sludge show similar findings [22], too. It should be worthwhile to revise the current approaches before extrapolating it to uninvestigated operational conditions.

Supplementary Materials: The following are available online at <http://www.mdpi.com/2073-4441/12/5/1249/s1>, Figure S1: Diffusion limitation with respect of oxygen penetration into the biofilm.

Author Contributions: Conceptualization, J.T. and M.C.; Methodology, J.T. and M.C.; Software, M.C.; Validation, M.C.; Formal Analysis, J.T.; Investigation, M.C.; Data Curation, M.C.; Writing—Original Draft Preparation, J.T. and M.C.; Writing—Review and Editing, J.T.; Visualization, M.C.; Supervision, J.T.; Project Administration, M.C.; Funding Acquisition, J.T. All authors have read and agreed to the published version of the manuscript.

Funding: This research was funded by the Federal Ministry for Education and Research [BMBF] grant number [FKZ WQ1361B].

Conflicts of Interest: The sponsors had no role in the design, execution, interpretation, or writing of the study.

Abbreviations

Nomenclature

A	surface area
ASM	activated sludge model
ASS	activated sludge system
b	decay rate
BF	biofilm
COD	chemical oxygen demand
D	diffusion coefficient
DO	dissolved oxygen
EBPR	enhanced biological phosphorus removal
f	residue factor
k	rate constant
L	characteristic length
n	number of
N	oxygen demand for nitrification
OUR	oxygen uptake rate
r	rate expression
S	dissolved fraction
SBR	sequence batch reactor
SBR-TFS	SBR-trickling filter system
SRT	sludge retention time
β	oxygen penetration factor
t	time
X	particulate fraction
Y	yield coefficient

Indices

0	initial
deg	degraded
E	endogenous residue
e	endogenous
eff	effluent
eli	elimination
ES	excess sludge
f	filtrated
F	fluid
H	heterotrophic organism
H+stor	degradation of heterotrophic organism and storage fraction
h	homogeneous
i	inert

i,BM	inert biomass residue
in	influent
N	nitrification
S	substrate
sp	specific
tot	total
U	unbiodegradable
US	ultra slow

References

- Daigger, G.T.; Grady, C.P.L. An assessment of the role of physiological adaptation in the transient response of bacterial cultures. *Biotechnol. Bioeng.* **1982**, *24*, 1427–1444. [[CrossRef](#)] [[PubMed](#)]
- Hood, M.A.; Guckert, J.B.; White, D.C.; Deck, F. Effect of nutrient deprivation on lipid, carbohydrate, DNA, RNA, and protein levels in *Vibrio cholerae*. *Appl. Environ. Microbiol.* **1986**, *52*, 788–793. [[CrossRef](#)] [[PubMed](#)]
- White, D. *Physiology and biochemistry of prokaryotes*; Oxford University Press: Oxford, UK, 2000.
- Morita, R.Y. *Bioavailability of Energy and the Starvation State*; Springer: Boston, MA, USA, 1993; pp. 1–23.
- Cebollero, E.; Reggiori, F.; Kraft, C. Reticulophagy and ribophagy: Regulated degradation of protein production factories. *Int. J. Cell Biol.* **2012**, *2012*, 1–9. [[CrossRef](#)] [[PubMed](#)]
- MacIntosh, G.C.; Bassham, D.C. The connection between ribophagy, autophagy and ribosomal RNA decay. *Autophagy* **2011**, *7*, 662–663. [[CrossRef](#)] [[PubMed](#)]
- Kurland, G.C.; Mikkola, R. *The Impact of Nutritional State on the Microevolution of Ribosomes, Starvation in Bacteria*; Kjelleberg, S., Ed.; Plenum Press: New York, NY, USA, 1993; pp. 225–237.
- Henze, M.; Gujer, W.; Van Loosdrecht, M.C.M.; Mino, T. *Activated sludge models ASM1, ASM2, ASM2d and ASM3*; IWA Publishing: London, UK, 2000.
- Wanner, O.; Gujer, W. A Multispecies Biofilm Model. *Biotechnol. Bioeng.* **1986**, *28*, 314–328. [[CrossRef](#)]
- Gikas, P.; Livingston, A.G. Specific ATP and specific oxygen uptake rate in immobilized cell aggregates: Experimental results and theoretical analysis using a structured model of immobilized cell growth. *Biotechnol. Bioeng.* **1997**, *55*, 660–673. [[CrossRef](#)]
- McKinney, R.E. Complete mixing activated sludge. *Water Sew. Work.* **1960**, *107*, 69.
- Gujer, W.; Henze, M.; Mino, T.; Loosdrecht, M.C.M. Van Activated sludge model No. 3. *Water Sci. Technol.* **1999**, *39*, 183–193. [[CrossRef](#)]
- Dold, P.L.; Ekama, G.; Marais, G.v.R. A General Model for the Activated Sludge Process. *Water Res. Public Heal. Eng.* **1980**, *12*, 47–77.
- Wanner, J.; Kucman, K.; Grau, P. Activated sludge process combined with biofilm cultivation. *Water Res.* **1988**, *22*, 207–215. [[CrossRef](#)]
- Wanner, O.; Morgenroth, E. Biofilm modeling with AQUASIM. *Water Sci. Technol.* **2004**, *49*, 137–144. [[CrossRef](#)] [[PubMed](#)]
- Spanjers, H.; Vanrolleghem, P. Respirometry as a tool for rapid characterization of wastewater and activated sludge. *Water Sci. Technol.* **1995**, *31*, 105–114. [[CrossRef](#)]
- Di Trapani, D.; Capodici, M.; Cosenza, A.; Di Bella, G.; Mannina, G.; Torregrossa, M.; Viviani, G. Evaluation of biomass activity and wastewater characterization in a UCT-MBR pilot plant by means of respirometric techniques. *Desalination* **2011**, *269*, 190–197. [[CrossRef](#)]
- Ramdani, A.; Dold, P.L.; Déléris, S.; Lamarre, D.; Gadbois, A.; Comeau, Y. Biodegradation of the endogenous residue of activated sludge. *Water Res.* **2010**, *44*, 2179–2188. [[CrossRef](#)] [[PubMed](#)]
- Tränckner, J.; Wricke, B.; Krebs, P. Estimating nitrifying biomass in drinking water filters for surface water treatment. *Water Res.* **2008**, *42*, 2574–2584. [[CrossRef](#)] [[PubMed](#)]
- Cramer, M.; Tränckner, J.; Schelhorn, P.; Kotzbauer, U. Degradation kinetics and COD fractioning of agricultural wastewaters from biogas plants applying biofilm respirometry. *Environ. Technol.* **2019**, *17*, 1–11. [[CrossRef](#)]
- Marais, G.v.R.; Ekama, G.A. The activated sludge process Part 1—Steady state behaviour. *Water S.A.* **1976**, *2*, 163–200.

22. Friedrich, M.; Takács, I.; Tränckner, J. Experimental Assessment of the Degradation of “Unbiodegradable” Organic Solids in Activated Sludge. *Water Environ. Res.* **2016**, *88*, 272–279. [[CrossRef](#)]
23. Friedrich, M.; Takács, I.; Tränckner, J. Physiological adaptation of growth kinetics in activated sludge. *Water Res.* **2015**, *85*, 22–30. [[CrossRef](#)]
24. Cramer, M.; Rinas, M.; Kotzbauer, U.; Tränckner, J. Surface contamination of impervious areas on biogas plants and conclusions for an improved stormwater management. *J. Clean. Prod.* **2019**, *217*, 1–11. [[CrossRef](#)]
25. Ye, L.; Hu, S.; Poussade, Y.; Keller, J.; Yuan, Z. Evaluating a strategy for maintaining nitrifier activity during long-term starvation in a moving bed biofilm reactor (MBBR) treating reverse osmosis concentrate. *Water Sci. Technol.* **2012**, *66*, 837–842. [[CrossRef](#)] [[PubMed](#)]
26. Buitrón, G.; Moreno-Andrade, I. Biodegradation kinetics of a mixture of phenols in a sequencing batch moving bed biofilm reactor under starvation and shock loads. *J. Chem. Technol. Biotechnol.* **2011**, *86*, 669–674. [[CrossRef](#)]
27. Cramer, M.; Tränckner, J.; Kotzbauer, U. Kinetic of denitrification and enhanced biological phosphorous removal (EBPR) of a trickling filter operated in a sequence-batch-reactor-mode (SBR-TF). *Environ. Technol.* **2019**, 1–10. [[CrossRef](#)]
28. Metcalf, E.; Eddy, M. *Wastewater Engineering: Treatment and Resource Recovery*; McGraw-Hill: New York, NY, USA, 2014.
29. Friedrich, M.; Takacs, I. A new interpretation of endogenous respiration profiles for the evaluation of the endogenous decay rate of heterotrophic biomass in activated sludge. *Water Res.* **2013**, *47*, 5639–5646. [[CrossRef](#)]
30. Dircks, K.; Pind, P.F.; Mosbæk, H.; Henze, M. Yield determination by respirometry—The possible influence of storage under aerobic conditions in activated sludge. *Water S.A.* **1999**, *25*, 69–74.
31. Kwok, W.K.; Picioreanu, C.; Ong, S.L.; Van Loosdrecht, M.C.M.; Ng, W.J.; Heijnen, J.J. Influence of biomass production and detachment forces on biofilm structures in a biofilm airlift suspension reactor. *Biotechnol. Bioeng.* **1998**, *58*, 400–407. [[CrossRef](#)]
32. Kuenen, J.G.; Jorgensen, B.B.; Revsbech, N.P. Oxygen Microprofiles of Trickling Filter Biofilms. *Water Res.* **1986**, *20*, 1589–1598. [[CrossRef](#)]
33. Viridis, B.; Read, S.T.; Rabaey, K.; Rozendal, R.A.; Yuan, Z.; Keller, J. Biofilm stratification during simultaneous nitrification and denitrification (SND) at a biocathode. *Bioresour. Technol.* **2011**, *102*, 334–341. [[CrossRef](#)]
34. Hauduc, H.; Rieger, L.; Oehmen, A.; van Loosdrecht, M.C.M.; Comeau, Y.; Héduit, A.; Vanrolleghem, P.A.; Gillot, S. Critical review of activated sludge modeling: State of process knowledge, modeling concepts, and limitations. *Biotechnol. Bioeng.* **2013**, *110*, 24–46. [[CrossRef](#)]



© 2020 by the authors. Licensee MDPI, Basel, Switzerland. This article is an open access article distributed under the terms and conditions of the Creative Commons Attribution (CC BY) license (<http://creativecommons.org/licenses/by/4.0/>).